J Mater Sci: Mater Med (2008) 19:2427–2435
DOI 10.1007/s10856-008-3368-7

The effects of peroxide content on the wear behavior, microstructure and mechanical properties of peroxide crosslinked ultra-high molecular weight polyethylene used in total hip replacement

Rizwan M. Gul

Received: 2 July 2007 / Accepted: 2 January 2008 / Published online: 25 January 2008

Abstract The wear of the ultra-high molecular weight polyethylene (UHMWPE) acetabular components and wear debris induced osteolysis are the major causes of failure in total hip replacements. Crosslinking has been shown to improve the wear resistance of UHMWPE by producing a network structure, resisting the plastic deformation of the surface layer. In this study organic peroxides were used to crosslink two different types of UHMWPE resins, using hot isostatic pressing as the processing method. The effects of peroxide content on the different properties were investigated, along with the effect of the crosslink density on the wear behavior. An increase in peroxide content decreases the melting point and the degree of crystallinity, which results in a decrease in the yield strength. The ultimate tensile strength remains essentially unchanged. The molecular weight between crosslinks decreases with an increase in the peroxide content and reaches a saturation limit at around 0.3–0.5 weight percent peroxide, its value at the saturation limit is a function of the virgin resin used for processing. The wear rate decreases linearly with the increase in crosslink density.

1 Introduction

Total hip replacement (THR), with articulating femoral head and acetabular cup, is widely performed to recover the functions of a hip joint when lost by severe arthritis. Ultra-high molecular weight polyethylene (UHMWPE) has been successfully used as acetabular components in THR for more than four decades; due to its high wear resistance, toughness, good bio-compatibility, and very low coefficient of friction [1–3]. However, wear of UHMWPE has been a significant problem with its use in this application [4, 5]. Crosslinking has been employed to improve the wear resistance, and several different types of commercially produced highly crosslinked UHMWPE acetabular cups are in clinical use [6–13]. Crosslinking produces a network structure resisting the uncoiling of the physical entanglements, and the formation of a highly oriented surface layer in the direction of sliding; a process which leads to the formation and release of wear debris [14–18].

Polyethylenes can be crosslinked by introducing free radicals on the polymer chain which initiate crosslinking: Three different methods are widely used [19, 20]. These three methods have also been employed to crosslink UHMWPE, the methods include: (1) by mixing the resin with organic peroxides and then heating the mixture [16, 21], (2) by using high energy radiation [6, 10, 13, 22–25], and (3) by grafting silane groups on the polymer chain and exposing it to increased humidity [26, 27].

Although the radiation crosslinked UHMWPE for use in THR have been extensively studied [6, 10, 13, 22–25], the peroxide crosslinked UHMWPE has not been that widely explored. The objective of this study was to investigate the effects of peroxide content on the processing, microstructure, crosslink density, mechanical properties and wear characteristics of the peroxide crosslinked UHMWPE. The other objective of this study was to explore the use of hot isostatic pressing (hipping) for processing peroxide crosslinked UHMWPE. The method is expected to be well suited for producing peroxide crosslinked UHMWPE, since the mixture can be kept at high temperature and pressure for a long time, and can lead to a well consolidated material

R. M. Gul (✉)
Department of Mechanical Engineering, NWFP University of Engineering and Technology, Peshawar, Pakistan
e-mail: rgul@alum.mit.edu

with the peroxides completely decomposed and reacted to form a uniformly crosslinked polymer.

2 Experimental

2.1 Materials

Two types of resins, Himont (or Montell) 1900 (Montell USA, Wilmington, DE) and GUR 1050 (Hoechst Celanese, League city, TX), were used in this study. GUR 1050 has a porous structure, while Himont 1900 is more condensed. The Himont 1900 resin has been reported to have a lower average molecular weight, a larger particle size and significantly higher degree of crystallinity. It may be mentioned here that Himont 1900 is no longer produced and the reactor that was used to create this resin has been dismantled [28].

Di-alkyl peroxides [$(R–OO)_nR'$] are commonly used for crosslinking polyethylene; selection of the proper peroxide from this group is critical to achieve efficient crosslinking and consolidation. At the processing temperature, the peroxide should have a half-life of at least a few minutes to avoid premature crosslinking which can cause incomplete consolidation. 2,5-Dimethyl-2,5-di-(*t*-butyl-peroxy)hexyne-3 (Peroxide 130), trade name Varox 130 (R. T. Vanderbilt Company, Norwalk, CT) was selected for the study, since it has one of the highest decomposition temperatures in the di-alkyl peroxide group. At the processing temperature used (210°C), it has a half-life of 0.26 min in Dodecane (its 10 h half life temperature is 131°C). At room temperature it is in liquid form and can be added directly to the resin. The chemical formula is:

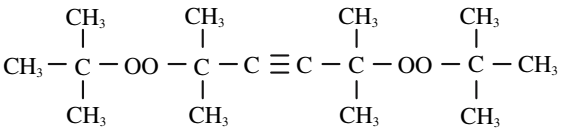

2,5-Dimethyl-2,5-di-(*tert*-butyl-peroxy)hexyne-3 (Peroxide 130)

2.2 Processing

Figure 1 shows all the steps in the production of the hot isostatic pressed samples. The apparatus used for hipping consisted of a pressure vessel in which the specimen was hipped, a furnace to heat the pressure vessel, a controller with a thermocouple to maintain the pressure vessel at constant temperature, and a nitrogen tank with a special regulator to apply the required pressure. A bleed valve was also present in the vessel to release excessive gas pressure produced during heating. The samples were hipped at 210°C and 13.8 MPa for 2 h, and then cooled in air at an approximate rate of 1°C/min. Table 1 lists the processing details for different samples. The Himont 1900 samples were soaked at 140°C for 1 h before heated to 210°C for final processing, while the GUR 1050 samples were heated directly to 210°C.

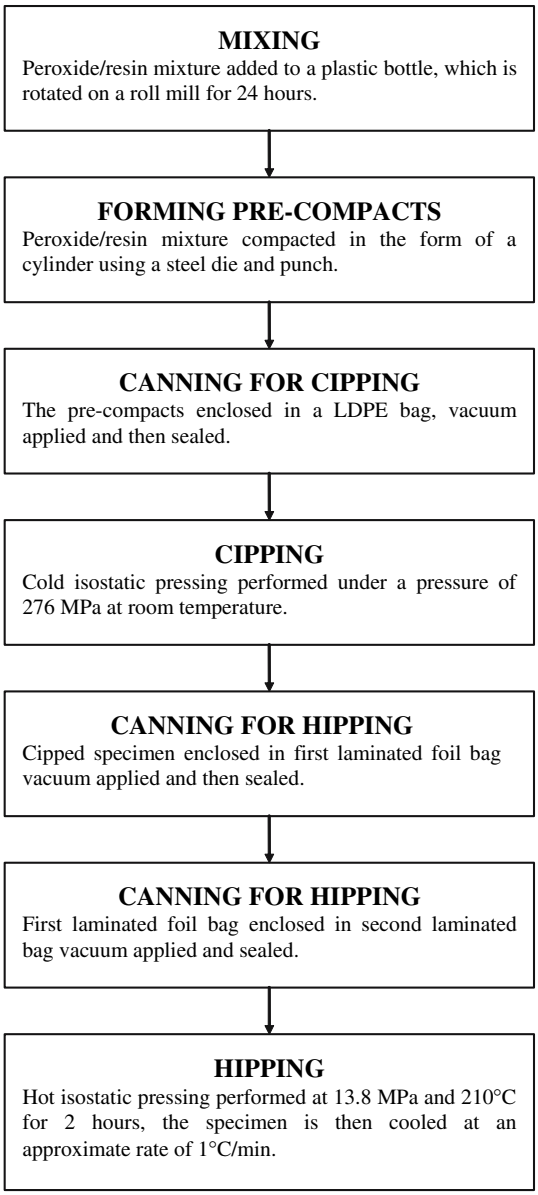

Fig. 1 Block diagram of different steps performed in the hot isostatic pressing of UHMWPE/peroxide mixture

2.3 Microscopy

Consolidation was assessed by light microscopy of thin sections, and by scanning electron microscopy (SEM) of the cryofractured samples. Thin sections (20 μm thick) of the consolidated materials were prepared by using a sledge microtome, and were analyzed using an Olympus BH2

Table 1 The peroxide content and other details of the different materials processed and analyzed in this study

Sample ID	Amount of peroxide in wt. %
Himont 1900 resin soaked at 140°C for 1 h before heated to 210°C for final processing	
0%-1900	0
0.15%-1900	0.15
0.3%-1900	0.3
0.5%-1900	0.5
1%-1900	1
2%-1900	2
GUR 1050 resin heated directly to 210°C	
0%-GUR 1050	0
0.1%-GUR 1050	0.1
0.2%-GUR 1050	0.2
0.25%-GUR 1050	0.25
0.3%-GUR 1050	0.3
0.35%-GUR 1050	0.35
0.4%-GUR 1050	0.4
0.45%-GUR 1050	0.45
0.5%-GUR 1050	0.5
0.7%-GUR 1050	0.7

(Olympus Optical Co., Tokyo, Japan) microscope under transmitted polarized light. To produce cryofractured surfaces, specimens 2–5 mm thick were submerged in liquid nitrogen, and fractured by pliers. The cryofractured surfaces obtained were gold-coated to be analyzed using a Stereoscan 240 (Cambridge Instruments, Cambridge, England) scanning electron microscope.

2.4 Thermal properties

Differential scanning calorimetry (DSC) was used to measure the thermal properties, such as, melting point and degree of crystallinity of the different samples. Perkin-Elmer model DSC 7a was used at a heating rate of 10°C/min. The heat of fusion of 100% crystalline polyethylene was taken as 289 J/g.

2.5 Crosslink density

Crosslink density and the molecular weight between crosslinks were calculated from the swell ratio, which was measured in a TMA set-up using a Perkin Elmer DMA7e. A 4 mm cube specimen, under a load of 20 mN was soaked in xylene, and then heated to 130°C at a rate of 5°C/min. The height of the specimen was measured with a quartz probe. The specimen swelled and its height reached a plateau after about 2.5 h. Then the force was reduced incrementally until the probe floated due to its buoyancy, and the final height was measured just before the probe floated. The crosslink density (υ_c) in moles per unit volume was calculated form the following equation [29, 30]:

$$\upsilon_c = -\frac{\ln(1-q^{-1}) + q^{-1} + \chi q^{-2}}{\overline{V_1} q^{-1/3}} \quad (1)$$

where q is the swell ratio, $\overline{V_1}$ is the partial volume of the diluent (xylene) and is 136 ml/mole, χ is the Flory–Huggins interaction parameter and is defined by the following equation: $\chi = 0.33 + 0.55/q$. Molecular weight between crosslinks (M_c) is calculated from the following:

$$M_c = \frac{\rho}{\upsilon_c} \quad (2)$$

where ρ, the density, is equal to the density of the amorphous polyethylene ($\rho \cong 0.862$ g/cm^3).

2.6 Tensile test

Tensile tests were performed on standard ASTM D638 dog-bone specimens, to measure the yield and ultimate tensile strength of the different samples. The dimensions of the narrow section were; length (or gage length) 9.53 mm, width 3.18 mm and thickness 2.54 mm. The overall length and width of the specimen were 50.8 mm and 9.53 mm. The radius of the fillet was 12.7 mm. An Instron 4505 testing machine was used, and the force was measured by a 10 KN load cell. The cross-head speed was 10 mm/min, producing a strain rate of 0.0175 s^{-1}. Four specimens were tested in each case. The tensile test was performed only on the GUR 1050 samples.

2.7 Wear test

A three pin, bi-directional, pin on disc wear testing machine simulating the physiological conditions in a hip joint was used to characterize the wear behavior. The details of the testing machine are discussed by Bragdon et al. [31]. The tests were conducted with serum as the lubricating medium. A Paul type load curve was used with a peak load of 267 N which resulted in a peak contact stress of 4.2 MPa. The pin traces a 5 × 10 mm rectangular path against the disc. The peak load occurs around one half of the rectangle. The preload, representing the swing phase of a gait, occurs around the other half. The test runs at a frequency of 2 Hz. Two or three 9 mm diameter polyethylene pins were cleaned and weighed at the beginning of

the test, after 0.5 million cycles and at the end of the test after 1 million cycles. The wear rate is measured as the decrease in the weight of the pin in mg divided by the number of cycles in millions.

3 Results

3.1 Consolidation

All the processed samples had uniform color which indicated good mixing of the peroxide and the resin. As the peroxide content was increased, the materials became more transparent and slightly yellow. Well consolidated materials were obtained at low peroxide contents, however, the consolidation decreased with the increase in peroxide content. This can be seen in the Himont 1900 samples from the cryofractured surfaces and light microscopy. The SEM micrographs of the cryofractured surfaces of 0%-1900 and 0.15%-1900 samples, displayed relatively smooth fracture surfaces (Fig. 2a and 2b). While in 0.5%-1900 and 2%-1900 samples (Fig. 2c and 2d), a star-burst morphology reflecting the powder flakes of the virgin resin emerged, and the roughness of the fracture surfaces increased. Large plastic deformation can still be observed in 0.5%-1900 sample, while the 2%-1900 sample's fracture surface was brittle with no plastic deformation. In GUR 1050 samples, although the consolidation decreased somewhat with an increase in peroxide content, the samples were better compacted than the 1900 samples.

3.2 Thermal properties

Table 2 shows the degree of crystallinity, onset melting point and peak melting temperature of all the materials, measured by the DSC analysis. In the Himont 1900 samples, the degree of crystallinity decreased with increasing peroxide content, and reached a plateau at around 0.5 wt.% peroxide content. As the peroxide content increased the onset melting point of the Himont 1900 specimens also decreased. The melting point is related with the lamellar thickness; thus the lamellar thickness decreased with increasing peroxide content. In addition to this, the melting peak became broader especially at high peroxide contents, as observed by the higher differences in the onset and peak

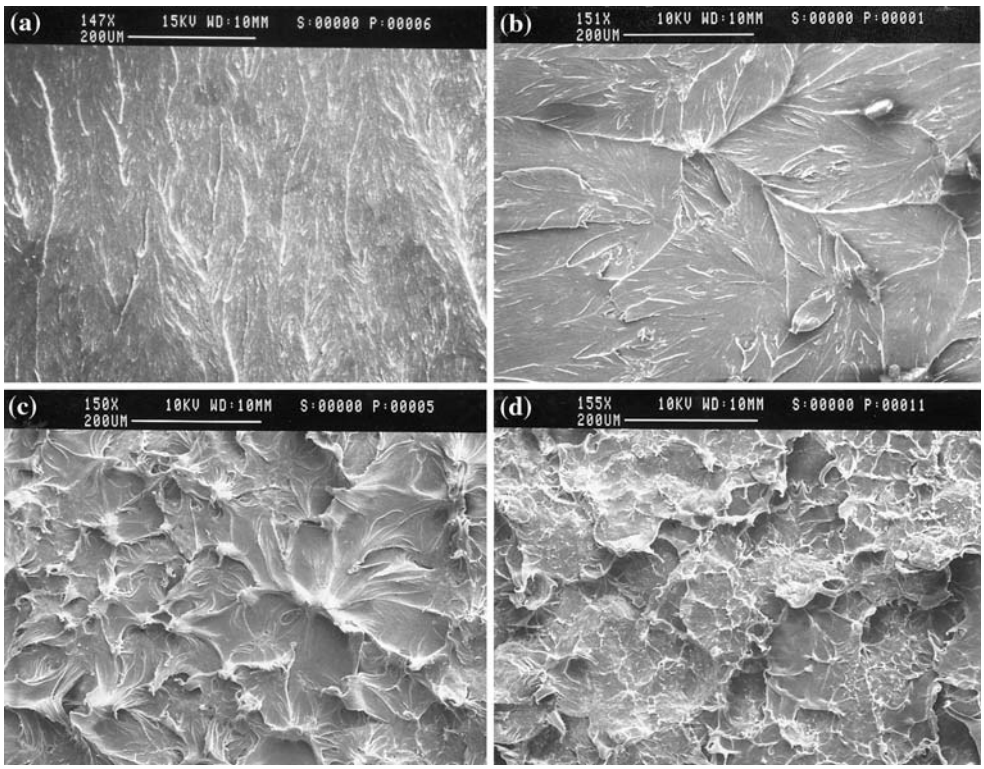

Fig. 2 SEM micrographs of the cryofractured surfaces of Himont 1900 resin with (**a**) 0 wt.%, (**b**) 0.15 wt.%, (**c**) 0.5 wt.% and (**d**) 2 wt.% peroxide content, respectively. The UHMWPE/peroxide mixture was soaked at 140°C for 1 h before heated to 210°C for final processing. No particle structure was observed in specimens with 0 wt.% and 0.15 wt.% peroxide content, while the observed particle structure in 0.5 wt.% and 2 wt.% peroxide content specimens reflects the powder flakes of the virgin resin

Table 2 Degree of crystallinity (%), onset melting point (°C) and peak melting temperature (°C) of different crosslinked samples, measured by the DSC analysis

Sample ID	Degree of crystallinity, (%)	Onset melting temperature, °C	Peak melting temperature, °C
0%-1900	58.9	128.9	139.5
0.15%-1900	51.6	124.9	133.4
0.3%-1900	49.6	121.7	131.7
0.5%-1900	48.4	117.3	127.4
1%-1900	48.8	112.6	125.8
2%-1900	45.9	106.9	120.8
0%-GUR 1050	51.0	125.6	135.4
0.1%-GUR 1050	45.4	121.0	130.8
0.2%-GUR 1050	43.8	119.3	128.0
0.25%-GUR 1050	43.2	118.4	127.4
0.3%-GUR 1050	43.4	117.8	126.1
0.35%-GUR 1050	41.8	117.5	125.1
0.4%-GUR 1050	42.2	116.8	124.3
0.45%-GUR 1050	41.2	116.9	124.0
0.5%-GUR 1050	41.4	115.8	123.3
0.7%-GUR 1050	40.4	114.5	122.0

The difference of the peak and onset melting temperatures provides an estimate for the width of the melting peak

melting temperatures. This represents a larger size range of crystallites. The results for GUR 1050 samples were similar to the Himont 1900 (Figs. 3 and 4). The crystallinity decreased and reached a plateau around 0.3–0.4 wt.% peroxide, while the onset melting point decreased continuously.

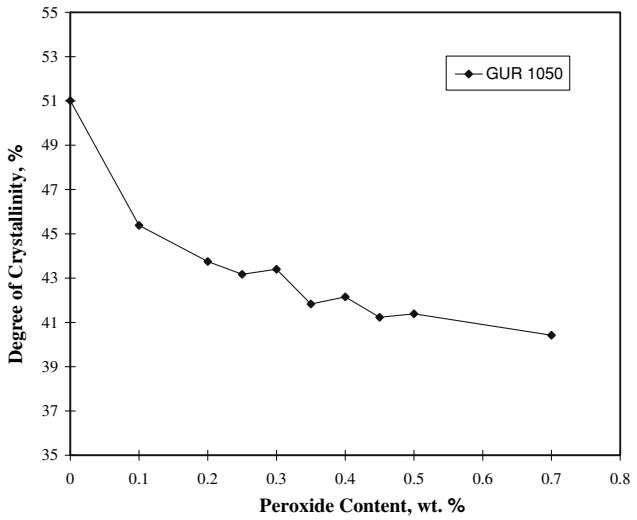

Fig. 3 Effect of peroxide content on the degree of crystallinity of the GUR 1050 samples, measured from the DSC analysis

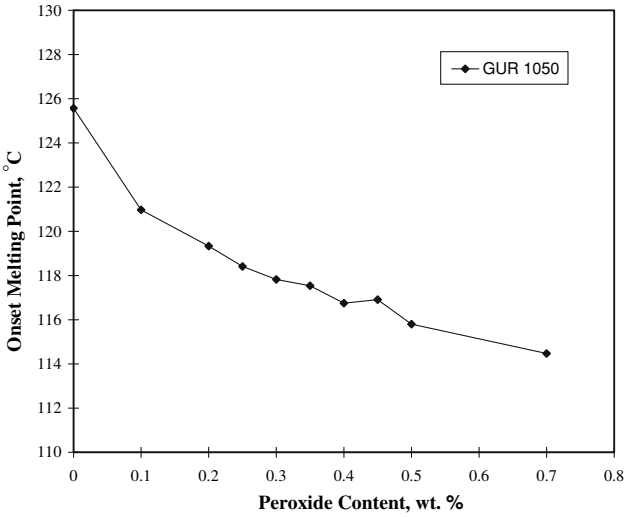

Fig. 4 Effect of peroxide content on the onset melting point of the GUR 1050 samples, measured from the DSC analysis

3.3 Crosslink density

The crosslink density and the molecular weight between crosslinks measured from the swelling experiment for different samples are shown in Table 3; while Fig. 5 shows the effect of peroxide content on the molecular weight between crosslinks for both Himont 1900 and GUR 1050 samples. As the peroxide increased the molecular weight between crosslinks decreased (the crosslink density increased), and reached a saturation limit. For the Himont 1900 samples, the saturation limit was observed at 0.5 wt.% peroxide. GUR 1050 samples show similar results: the molecular weight between crosslinks decreased and reached a plateau at about 0.3–0.4 wt.% peroxide. A similar plateau was also observed in the decrease in crystallinity content. The molecular weight between crosslinks at the saturation limit in the GUR specimens was lower than in the Himont 1900 specimens; the crosslink density was higher.

3.4 Tensile properties

Figures 6 and 7 show the effect of the peroxide content on the yield strength and ultimate tensile strength (UTS) of GUR 1050 samples, respectively. The yield strength, as measured at the zero slope condition, decreased with the increase in peroxide content. The decrease in the yield strength was directly proportional to the decrease in degree of crystallinity of these samples ($R^2 = 0.9813$). The ultimate tensile strength did not change much with the increase in peroxide content; similar observation has been made in previous studies [32]. The peroxide crosslinked specimens had slightly smaller UTS than the control specimen (0%-GUR 1050).

Table 3 Volume swell ratio, molecular weight between crosslinks and crosslink density of different samples, measured by the swelling experiment

Sample ID	Volume swell ratio, mm^3/mm^3	Mol. Wt. between crosslinks, g/mole	Crosslink density, $moles/m^3$
0%-1900	No Plateau	–	–
0.15%-1900	4.54	10637	81.0
0.3%-1900	4.08	8996	95.8
0.5%-1900	3.32	6416	134.4
1%-1900	3.31	6391	134.9
2%-1900	3.19	6003	143.6
0%-GUR 1050	No Plateau	–	–
0.1%-GUR 1050	3.54	7158	120.5
0.2%-GUR 1050	3.24	6183	139.4
0.25%-GUR 1050	3.35	6540	131.8
0.3%-GUR 1050	2.97	5295	162.8
0.35%-GUR 1050	2.94	5180	166.4
0.4%-GUR 1050	2.81	4783	180.2
0.45%-GUR 1050	2.93	5147	167.5
0.5%-GUR 1050	2.94	5199	165.8
0.7%-GUR 1050	2.92	5133	168.0

The swell ratio is measured from the change in height of a 4 mm cube specimen immersed in xylene at 130°C

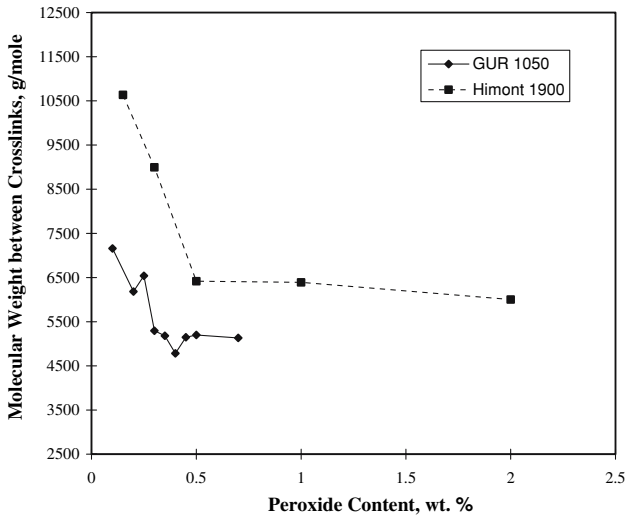

Fig. 5 Effect of peroxide content on the molecular weight between crosslinks of the GUR 1050 and Himont 1900 samples, measured from the swelling experiment. The volume swell ratio is measured from the change in height of a 4 mm cube specimen soaked in xylene at 130°C

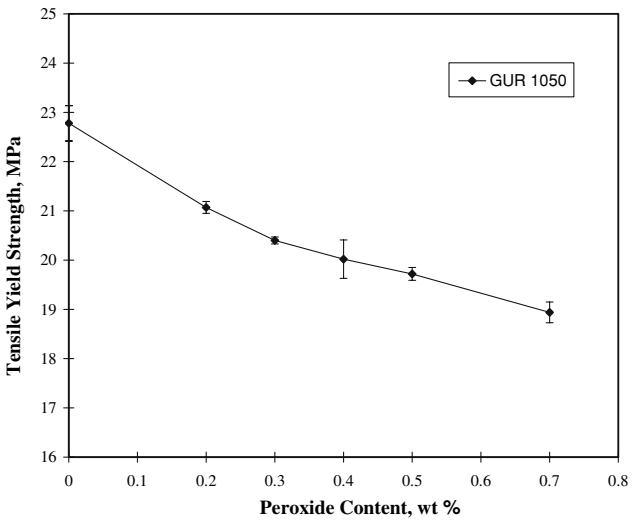

Fig. 6 Effect of peroxide content on the tensile yield strength (MPa) of the different GUR 1050 samples. The yield strength is measured at the zero slope condition

3.5 Wear characteristics

The effect of peroxide content on the bi-directional pin on disc wear behavior of both Himont 1900 and GUR 1050 specimens are presented in Fig. 8. The wear rate decreased considerably with the addition of even a small amount of peroxide in both cases. The wear rate decreased further with the increase in peroxide content, and reached a saturation limit in the GUR 1050 samples. At the same peroxide content, the wear resistance of GUR 1050 samples was significantly higher than the Himont 1900 samples.

4 Discussion

Hot isostatic pressing has been successfully used in this study to process well consolidated peroxide crosslinked materials, using suitable heating and processing parameters. The degree of consolidation decreased with the increase in peroxide content in both Himont 1900 and GUR 1050 samples. This decline in the degree of consolidation can be explained as follows; during the mixing of the peroxide and the resin, the peroxide deposits around the particle boundaries. When this mixture is heated, some of the peroxide will decompose on the boundaries instead of

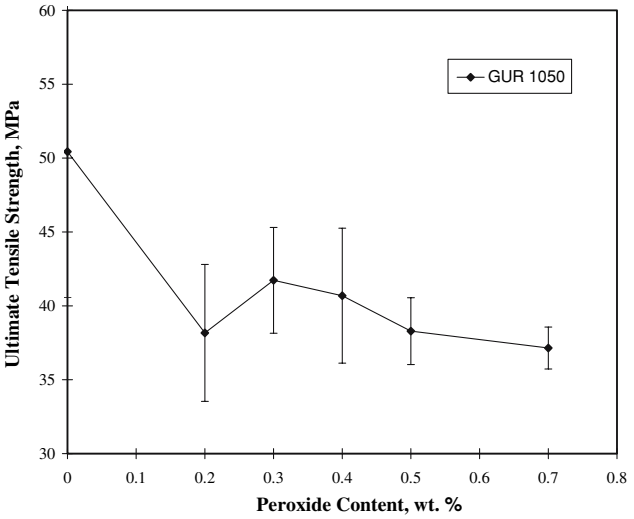

Fig. 7 Effect of peroxide content on the ultimate tensile strength (MPa) of the different GUR 1050 samples

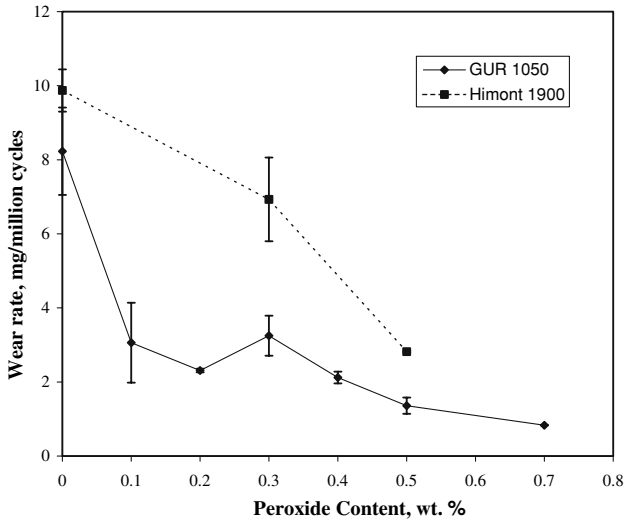

Fig. 8 Effect of peroxide content on the wear rate (mg/million cycles) of the GUR 1050 and Himont 1900 samples. The wear rate is measured after 1 million cycles using a bi-directional pin on disc wear testing machine simulating the conditions in a hip joint

diffusing into the particles. As the peroxide content increases the relative amount of decomposition on the particle boundaries will increase. The decomposition products form voids leading to the poor consolidation. In addition, the boundaries will be prematurely crosslinked making the material more difficult to process. The phenomenon may be augmented in the Himont 1900 samples by the 1 h soaking time at 140°C before heating the specimen to 210°C. At this temperature plateau the peroxide may have decomposed on the boundaries causing premature crosslinking and poor compaction at the processing temperature of 210°C. GUR 1050 samples showed relatively better consolidation than the Himont 1900 samples at the same peroxide content. This better consolidation can be due to the smaller particle size of the GUR resin combined with its more diffuse structure promoting an even and uniform distribution of the peroxides, and resulting in better consolidation. Secondly the GUR 1050 specimens were heated directly to 210°C (without any plateau at 140°C) which may avoid premature crosslinking and giving a more consolidated material.

In both the Himont 1900 and GUR 1050 samples, the degree of crystallinity decreased with increasing peroxide content and reached a plateau, which may reflect the formation of a complete crosslink network. The observed decrease agrees with previous studies [30, 32–34], and shows how crystal growth is inhibited by the crosslinks. They restrict chain mobility and act as local defects that cannot be accommodated in the crystals. As the peroxide content increases, the onset melting point of the specimens decreases. Thus, the lamellar thickness decreases, due to the reduction in the size of chain segments which can crystallize. In addition, the difference between onset and peak melting temperatures also increased at high peroxide contents in Himont 1900 samples, implying a larger size range of the crystallites. It was discussed in the last paragraph that at high peroxide contents the consolidation degrades rapidly because of the premature crosslinking on the particle boundaries. This implies that the boundaries will have a larger degree of crosslinking compared to the particle centers, which causes a larger size range of crystallites and a broader peak in the Himont 1900 samples.

Similar to the results of the degree of crystallinity, the crosslink density increased with the increase in peroxide content and reached a saturation limit at 0.5 wt.% peroxide for Himont 1900 samples, and 0.3–0.4 wt.% peroxide for GUR 1050 samples. The limit may represent a complete crosslink network and the fulfillment of all the entanglement and branch sites available for crosslinking. It occurs at the same peroxide concentration where the saturation in the degree of crystallinity was observed. Since the wear resistance is expected to be proportional to the crosslink density, the wear behavior should improve with the increase in peroxide content and reach a saturation limit at the completion of the crosslink network. The molecular weight between crosslinks at the saturation limit in the case of GUR 1050 specimens is lower as compared to the Himont 1900 specimens; the crosslink density is higher. According to Posthuma et al. [34] the crosslinking of polyethylene in solution is produced by a cage mechanism; involving the decomposition of peroxide at the moment when two segments of polymer molecules form a cage surrounding the peroxide molecule. One consequence of this mechanism is that crosslinking takes place preferentially at the entanglement sites, since there the segments are

in close proximity. The increased crosslink density achieved in GUR 1050 samples can be due to the higher physical entanglement density of the GUR resin because of its higher average molecular weight. The other probable reason is the higher branch content in the GUR resin.

The yield strength of the GUR 1050 samples decreased linearly with the decrease in the degree of crystallinity, due to the increase in peroxide content. This is due to the fact that crystallites are the principle source of rigidity, and it will be easier to yield (flow) a specimen with a smaller number and size of crystalloids [35, 36]. The minor change in the UTS of the GUR 1050 samples with increasing peroxide content can be explained on the basis of two opposing mechanisms: The UTS is expected to increase due to the increased resistance of chemical crosslinks to molecular mobility at large deformations, while the UTS is expected to decrease due to the decrease in the number of crystallites which act as physical entanglements. These two opposing tendencies, produced by the increase in the number of crosslinks and decrease in the degree of crystallinity with increasing peroxide content, result in the absence of any correlation between the UTS and the peroxide content.

A significant difference in the values of the wear rate for different materials is evident. Crosslinking significantly decreases wear rate in both materials. The wear rate appears to follow the same changes as a function of the peroxide content, as observed in the crosslink density. At the same peroxide content GUR 1050 samples show higher wear resistance than Himont 1900 samples, in agreement with the observance of higher crosslink densities in the GUR 1050 samples. The plot of the wear rate as a function of the molecular weight between crosslinks (Fig. 9) shows that the wear rate decreases linearly as the molecular weight between crosslinks decreases.

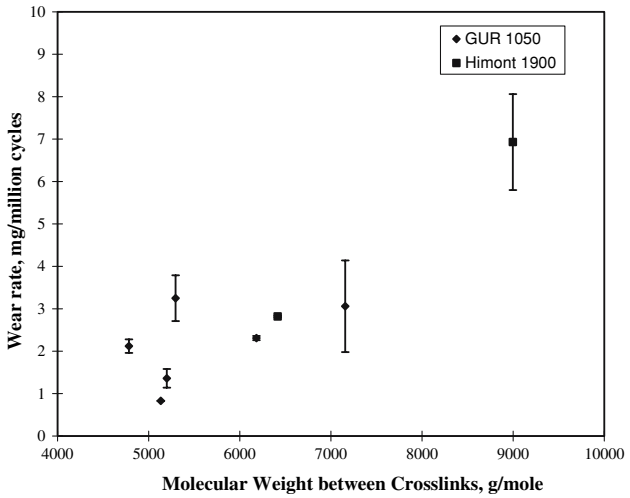

Fig. 9 Effect of molecular weight between crosslinks (g/mole) on the wear rate (mg/million cycles) of different peroxide crosslinked samples. A linear relationship exists between the molecular weight between crosslinks and the wear rate

Wear mechanisms in total joint replacements are divided in two categories; adhesion and abrasion, and surface fatigue wear. The resistance to adhesive and abrasive wear is directly related to the shear strength of the surface layer, while the resistance to the surface fatigue wear is related to the elongation at break and toughness. The shear strength of the surface layer can be increased by increasing the number of physical entanglements in an uncrosslinked material and by increasing the crosslink density in a crosslinked material. It will be larger in a crosslinked material as compared to an uncrosslinked material. The chemical crosslinks will obstruct the plastic deformation of the surface layer by resisting the uncoiling of the entanglements; a process necessary for large deformations and the formation of wear debris. The magnitude of the decrease in adhesive and abrasive wear will be proportional to the decrease in molecular weight between crosslinks. Since the test setup used in this study produces wear mainly by adhesion and abrasion, the wear was expected to decrease linearly with the molecular weight between crosslinks: as demonstrated by the experiments.

Radiation crosslinked wear resistant UHMWPE is now widely used in acetabular components for THR. However, some possible problems identified with the use of these materials include lower mechanical properties and fatigue resistance. Peroxide crosslinking provide an alternate route to get higher wear resistance with a different set of mechanical properties. Moreover, since peroxide crosslinking is done in the melt sate, no post-irradiation thermal treatment will be required which is indispensible for most radiation crosslinked UHMWPE, to eliminate the free radicals. The possible drawbacks of peroxide crosslinked UHMWPE include the presence of by-products of the chemical reaction and long term oxidative degradation.

5 Conclusions

Hot isostatic pressing is a well suited technique for producing peroxide crosslinked UHMWPE. The peroxide/resin mixture can be kept at high temperatures and pressures for long times, under vacuum, and can lead to a well consolidated material with peroxides completely decomposed and reacted to form a uniformly crosslinked material. This study shows that by using suitable heating and processing parameters, peroxide crosslinked material with high degree of consolidation can be fabricated by hipping. However, the consolidation may degrade at higher peroxide contents. Mixing of the peroxide and the resin is satisfactory, in spite of the fact that no solvent was used to aid dispersion.

The degree of crystallinity and the onset melting point decrease with an increase in peroxide content, suggesting that both the number and the size of the crystallites are decreasing. The crystallinity reaches a plateau at the higher peroxide contents. The crosslink density increases with the peroxide content and reaches a saturation limit at around 0.3–0.5 wt.% peroxide. The crosslink density at this limit is a function of the virgin resin used for processing, and increases with the increase in average molecular weight, branch content and entanglement density of the virgin resin. Tensile test shows that the yield strength decreases linearly with a decrease in the degree of crystallinity caused by increasing peroxide content. However, the ultimate tensile strength does not change much as the peroxide content is increased.

The wear rate decreases drastically as the peroxide content increases. At the same peroxide content GUR 1050 samples show lower wear rate than the Himont 1900 samples. The decrease in wear rate is linear to the decrease in molecular weight between crosslinks. This observation supports the hypothesis that the wear can be reduced by increasing the shear strength of the surface layer, by producing chemical crosslinks resisting the uncoiling of the entanglements.

Acknowledgement The author would like to acknowledge the effective support and guidance of Prof. F. J. McGarry, Department of Materials Science and Engineering, Massachusetts Institute of Technology, Cambridge, MA in completing the study and preparing the manuscript.

References

1. S.M. Kurtz, O.K. Muratoglu, M. Evans, A.A. Edidin, Biomaterials **20**, 1659 (1999)
2. S. Li, Opera. Techn. Orthop. **11**, 288 (2001)
3. L.A. Pruitt, Biomaterials **26**, 905 (2005)
4. W.H. Harris, Clin. Orthop. Relat. Res. **311**, 46 (1995)
5. A. Buford, T. Goswami, Mater. Design **25**, 385 (2004)
6. N. Shibata, S.M. Kurtz, N. Tomita, J. Biomech. Sci. Eng. **1**, 107 (2006)
7. M. Jasty, H.E. Rubash, O. Muratoglu, J. Arthroplasty **20**, 55 (2005)
8. M.D. Ries, J. Arthroplasty **20**, 59 (2005)
9. D.W. Manning, P.P. Chiang, J.M. Martell, J.O. Galante, W.H. Harris, J. Arthroplasty **20**, 880 (2005)
10. O.K. Muratoglu, C.R. Bragdon, D.O. O'Connor, M. Jasty, W.H. Harris, J. Arthroplasty **16**, 149 (2001)
11. J.M. Martell, J.J. Verner, S.J. Incavo, J. Arthroplasty **18**, 55 (2003)
12. O.K. Muratoglu, C.R. Bragdon, D.O. O'Connor, M. Jasty, W.H. Harris, R. Gul, F. McGarry, Biomaterials **20**, 1463 (1999)
13. G. Lewis, Biomaterials **22**, 371 (2001)
14. N.P. Suh, *Tribophysics* (Prentice-Hall, Inc., NJ, 1986) p. 223
15. R.M. Gul, F.J. McGarry, C.R. Bragdon, O.K. Muratoglu, W.H. Harris, Biomaterials **24**, 3193 (2003)
16. S.M. Kurtz, L.A. Pruitt, C.W. Jewett, J.R. Foulds, A.A. Edidin, Biomaterials **20**, 1449 (1999)
17. A. Wang, Wear **248**, 38 (2001)
18. A.A. Edidin, L. Pruitt, C.W. Jewett, D.J. Crane, D. Roberts, S.M. Kurtz, J. Arthroplasty **14**, 616 (1999)
19. B. Dave, in *Handbook of Elastomers: New Developments and Technology*, ed. by A.K. Bhomick, H.L. Stephens (Marcel Dekker, Inc, 1988)
20. S. Venkatraman, L. Kleiner, Adv. Polym. Technol. **9**, 265 (1989)
21. F.W. Shen, H.A. Mckellop, R. Salovey, J. Polym. Sci. Part B: Polym. Phys. **34**, 1063 (1996)
22. H. Oonishi, Y. Takayama, E. Tsuji, Radiat. Phys. Chem., Int. J. Radiat. Appl. Instrum., Part C **39**, 495 (1992)
23. H. Oonishi, M. Kuno, E. Tsuji, A. Fujisawa, J. Mater. Sci.-Mater. M. **8**, 11 (1997)
24. O.K. Muratoglu, D.O. O'Connor, C.R. Bragdon, J. Delaney, M. Jasty, W.H. Harris, E. Merrill, P. Vengupalan, Biomaterials **23**, 717 (2002)
25. S.M. Kurtz, M.L. Villarraga, M.P. Herr, J.S. Bergstrom, C.M. Rimnac, A.A. Edidin, Biomaterials **23**, 3681 (2002)
26. C.Y. Tang, X.L. Xie, X.C. Wu, R.K.Y. Li, Y.W. Mai, J. Mater. Sci.-Mater. M **13**, 1065 (2002)
27. H. Sakoda, A.M. Voice, H.M.J. McEwen, G.H. Issac, C. Hardaker, B.M. Wroblewski, J. Fisher, J. Arthroplasty **16**, 1018 (2001)
28. S.M. Kurtz, in *The UHMWPE Handbook: Ultra-High Molecular Weight Polyethylene in Total Joint Replacement* (Elsevier Academic Press, 2004) p. 17
29. R.M. Gul, Ph. D Thesis, Department of Materials Science and Engineering, Massachusetts Institute of Technology (1997)
30. D.J. Dijkstra, W. Hoogsteen, A.J. Pennings, Polymer **30**, 866 (1989)
31. C.R. Bragdon, D.O. O'Connor, J.D. Lowenstein, M. Jasty, S.A. Biggs, W.H. Harris, J. Arthroplasty **16**, 658 (2001)
32. J. de Boer, A.J. Pennings, Polymer **23**, 1944 (1982)
33. J. de Boer, H.-J. den Berg, A.J. Pennings, Polymer **25**, 513 (1984)
34. A. Posthuma, J. de Boer, A.J. Pennings, J. Polym. Sci. Part B Polym. Phys. **14**, 187 (1976)
35. C.I. Yim, K.J. Lee, J.Y. Jho, K. Choi, Polym. Bull. **42**, 433 (1999)
36. H.A. Khonakdar, J. Morshedian, U. Wagenknecht, S.H. Jafari, Polymer **44**, 4301 (2003)